Global Change Biology

Global Change Biology (2016) **22**, 2238–2254, doi: 10.1111/gcb.13221

Soil–plant–atmosphere conditions regulating convective cloud formation above southeastern US pine plantations

GABRIELE MANOLI[1], JEAN-CHRISTOPHE DOMEC[1,2], KIMBERLY NOVICK[3], ANDREW CHRISTOPHER OISHI[4], ASKO NOORMETS[2], MARCO MARANI[1] and GABRIEL KATUL[1]

[1]*Nicholas School of the Environment, Duke University, Durham, NC 27708, USA,* [2]*Department of Forestry and Environmental Resources, North Carolina State University, Raleigh, NC 27607, USA,* [3]*School of Public and Environment Affairs, Indiana University, Bloomington, IN 47405, USA,* [4]*Coweeta Hydrologic Laboratory, USDA Forest Service, Otto, NC 28763, USA*

Abstract

Loblolly pine trees (*Pinus taeda* L.) occupy more than 20% of the forested area in the southern United States, represent more than 50% of the standing pine volume in this region, and remove from the atmosphere about 500 g C m^{-2} per year through net ecosystem exchange. Hence, their significance as a major regional carbon sink can hardly be disputed. What is disputed is whether the proliferation of young plantations replacing old forest in the southern United States will alter key aspects of the hydrologic cycle, including convective rainfall, which is the focus of the present work. Ecosystem fluxes of sensible (H_s) and latent heat (LE) and large-scale, slowly evolving free atmospheric temperature and water vapor content are known to be first-order controls on the formation of convective clouds in the atmospheric boundary layer. These controlling processes are here described by a zero-order analytical model aimed at assessing how plantations of different ages may regulate the persistence and transition of the atmospheric system between cloudy and cloudless conditions. Using the analytical model together with field observations, the roles of ecosystem H_s and LE on convective cloud formation are explored relative to the entrainment of heat and moisture from the free atmosphere. Our results demonstrate that cloudy–cloudless regimes at the land surface are regulated by a nonlinear relation between the Bowen ratio Bo $= H_s/\mathrm{LE}$ and root-zone soil water content, suggesting that young/mature pines ecosystems have the ability to recirculate available water (through rainfall predisposition mechanisms). Such nonlinearity was not detected in a much older pine stand, suggesting a higher tolerance to drought but a limited control on boundary layer dynamics. These results enable the generation of hypotheses about the impacts on convective cloud formation driven by afforestation/deforestation and groundwater depletion projected to increase following increased human population in the southeastern United States.

Keywords: convective clouds, forest ecosystem, land-cover change, soil–plant–atmosphere interactions

Received 26 October 2015 and accepted 9 December 2015

Introduction

The southern United States, particularly its southeastern (SE) region, includes some of the most intensively managed forests worldwide (Hansen *et al.*, 2013). Currently, planted pines are at some 14 million hectares, occupy about 20 percent of the entire forested area of the southern U.S. Loblolly pines (*Pinus taeda* L.), and represent more than 50% of the standing pine volume within the SE (Little, 1971; Baker & Langdon, 1990). There is also broad agreement within the FluxNet records complemented by several model calculations and biometric estimates that these pine plantations contribute to the removal of around 500 g C m^{-2} per year as net ecosystem CO_2 exchange with the atmosphere (e.g. Schäfer *et al.*, 2003; Churkina *et al.*, 2005; Siqueira *et al.*, 2006; Stoy *et al.*, 2006ab; Friend *et al.*, 2007; Noormets *et al.*, 2010; Novick *et al.*, 2015).

Current economic models predict an increase in pine plantation area within the SE by industry and private owners, in part due to federal policies aimed at reducing timber harvesting from western forests (Wear & Greis, 2012) and more recently to the potential use of coarse woody debris after harvest as biofuel (Frederick *et al.*, 2008; Wear & Greis, 2012). Over the last 50 years, this expansion primarily replaced natural and thus older pine forests (together with mixed hardwoods and wetlands) with younger and faster growing Loblolly pines. Given the projected regional scale of this land-cover change, future water resources planning

*Correspondence: Gabriele Manoli, tel. +1 919-613-8033, fax +1 919-684-8741, e-mail: gabriele.manoli@duke.edu

for the SE cannot ignore the rapid areal expansion of pine plantations (Jackson *et al.*, 2008), including the possibility that such changes may alter the hydrologic cycle, including the precipitation regime. Age-related differences in evapotranspiration (ET) between old and young trees can in fact be significant: the mean ET of a 35-year-old pine forest located in the Piedmont region of North Carolina (NC) is estimated in this study to be 640 ± 40 [mm yr^{-1}], and for similar climatic conditions, younger pine plantations in NC revealed much higher ET fluxes. Specifically, Stoy *et al.* (2006a,b) and Domec *et al.* (2012) reported values of 753 ± 125 and 980 ± 46 [mm yr^{-1}] for a 19-year and 5-year-old Loblolly pine stands, respectively, in NC.

The main precipitation mechanism likely to be impacted by any large-scale land-cover changes is convective rainfall. In the SE, this type of rainfall occurs mostly during the growing season and is sensitive to alterations in ecosystem level heat and moisture exchange rates (Juang *et al.*, 2007a,b) when they occur on spatial scales much larger than the boundary layer height (~1000–2000 m). Changes in vegetation age, for example, due to typical clear-cut rotations every 20–25 years, alter vegetation structure, including canopy leaf area, and thus affect the hydraulic control of vegetation on transpiration, leading to changes in the partitioning of sensible and latent heat fluxes at the land surface. In addition, the projected increase in human population can increase groundwater depletion, thus altering the ecosystem fluxes of moisture, especially in coastal regions where root water uptake mechanisms rely on a shallow water table (Domec *et al.*, 2012; Manoli *et al.*, 2014; Bonetti *et al.*, 2015).

While there is consensus on the coupling between root-zone soil moisture and precipitation (Salvucci *et al.*, 2002; Findell & Eltahir, 2003; Koster *et al.*, 2004; Wu *et al.*, 2007; Wei *et al.*, 2008), the debate continues on the pathways by which this coupling is achieved (Guillod *et al.*, 2015). The aforementioned coupling remains an issue because of the numerous nonlinear feedback mechanisms between soil moisture content, ecosystem level heat, and moisture exchange rates, and the slowly evolving large-scale free atmospheric (FA) states existing above the atmospheric boundary layer (ABL). Moreover, the role of biotic factors controlling the ecosystem fluxes of sensible H_s and latent LE heat in pine plantations vs. abiotic controls associated with large-scale entrainment of heat and water vapor (Siqueira *et al.*, 2009; Taylor *et al.*, 2012; Williams *et al.*, 2012) must be addressed. To date, these issues are investigated by climate (e.g. Williams *et al.*, 2012), land surface (e.g. Maxwell *et al.*, 2007; Kollet & Maxwell, 2008; Sanchez-Mejia & Papuga, 2014; Bonetti *et al.*, 2015), and atmospheric (e.g. Ban-Weiss *et al.*, 2011) models attempting to capture the full complexity of the ABL processes including radiative transfer, turbulence, cloud micro-physics, and evapotranspiration. In parallel, it has been shown that zero-order mixed-layer dynamics reasonably describe the diurnal evolution of the ABL (Tennekes, 1973; Tennekes & Driedonks, 1981; Driedonks, 1982; Kim & Entekhabi, 1998; Pino *et al.*, 2006; Stevens, 2006; Porporato, 2009; Schalkwijk & Jonker, 2013), thus prompting interest in their potential use for the problem at hand.

The main objective of this study is to delineate the free atmospheric (FA) states for which biotic processes within pine plantations exert a significant control on convective cloud formation. Specifically, we aim at deriving a zero-order model for SE pine plantations that describes the transition between cloudy and cloudless regimes accounting for biotic (associated with soil–plant controls on H_s and LE) and abiotic controls associated with FA sources. It is envisaged that with such a model, the impact of major land-cover transformations, such as the expansion of pine plantations (along with their age-related changes) in the SE, on convective rainfall occurrences could complement other assessments for albedo effects, carbon sequestration, and warming potential. Cloud formation could also provide interesting ecophysiological feedback mechanisms, reducing incoming radiation and thus photosynthesis, temperature, and temperature-dependent processes like respiration.

The focus here is on convective cloud formation as defined by the crossing between the ABL height and the lifting condensation level (LCL). While convective rainfall is not the only rainfall mechanism in the SE (Ramírez-Cobo *et al.*, 2011), it does contribute to a significant portion of the summertime rainfall, when the productivity of Loblolly pine plantations is highest (Juang *et al.*, 2007a). With regard to the cloud formation mechanism, a crossing between ABL height and LCL determines the formation of shallow stratocumuli (Stevens, 2006) and represents a necessary (although not sufficient) condition for initiating convective rainfall (Juang *et al.*, 2007a,b). When LCL and ABL do cross, several other conditions must be satisfied to initiate convective rainfall. However, clear-sky conditions (and thus no rain) are certain when the ABL does not cross the LCL. In other terms, this work does not attempt to describe all the processes involved in rainfall triggering, but focuses on the minimum necessary conditions that must be satisfied to establish cloud formation and predisposition to convective rainfall. This minimum set of conditions can be explored with a slab ABL model and associated temperature and humidity budgets in the atmosphere (Juang *et al.*, 2007a,b; Siqueira *et al.*, 2009; Konings *et al.*, 2010; Bonetti *et al.*, 2015). The 'metric of success' is whether cloud formation can be described from FA conditions and minimal parametrization of the biotic controls on ecosystem H_s and LE (or their ratio) in Loblolly pine plantations varying in age and canopy structure within the SE.

Materials and methods

Study sites

To investigate biotic controls on convective cloud formation, data from four Loblolly pine plantations are considered as case studies (see Figs 1 and 2 and Table 1). The first site is a 22-year-old stand (at the time of data collection, in 2005) situated within the Blackwood division of the Duke Forest near Durham, North Carolina (US-Dk3 in the Ameriflux database). The second is also a plantation (established in 1992) situated in the lower coastal plain of North Carolina (US-NC2 in the Ameriflux database). The two sites were selected for (i) the availability of sounding data from nearby airports and (ii) their similar characteristics (same pine species, similar climate) but different soil types and water supply to the roots. The soil texture is mostly clay at the Duke Forest site (Juang *et al*., 2007b) but is predominantly Belhaven series histosol over coarse sand at the Coastal site (Domec *et al*., 2012). The rooting depth at the Coastal plantation site is 2 m , which is much deeper than the rooting depth at the Duke Forest pine plantation site where the root-zone depth is restricted to around 0.3 m (Oren *et al*., 1998) due to the presence of a hard clay pan. The deep rooting depth at the Coastal site allows direct access to the water table (between 1 and 2 m below the soil surface) as discussed elsewhere (Noormets *et al*., 2010; Domec *et al*., 2012; Manoli *et al*., 2014). Details on the location, experimental setup and data collection procedures are described elsewhere (Stoy *et al*., 2005; Juang *et al*., 2007a; Sun *et al*., 2010; Domec *et al*., 2012). Both sites were instrumented with Eddy covariance systems and soil moisture sensors.

To evaluate the role of stand age on the partitioning of surface energy fluxes, two additional sites have been considered: a Young and an Old plantation (Fig. 2). The Young plantation

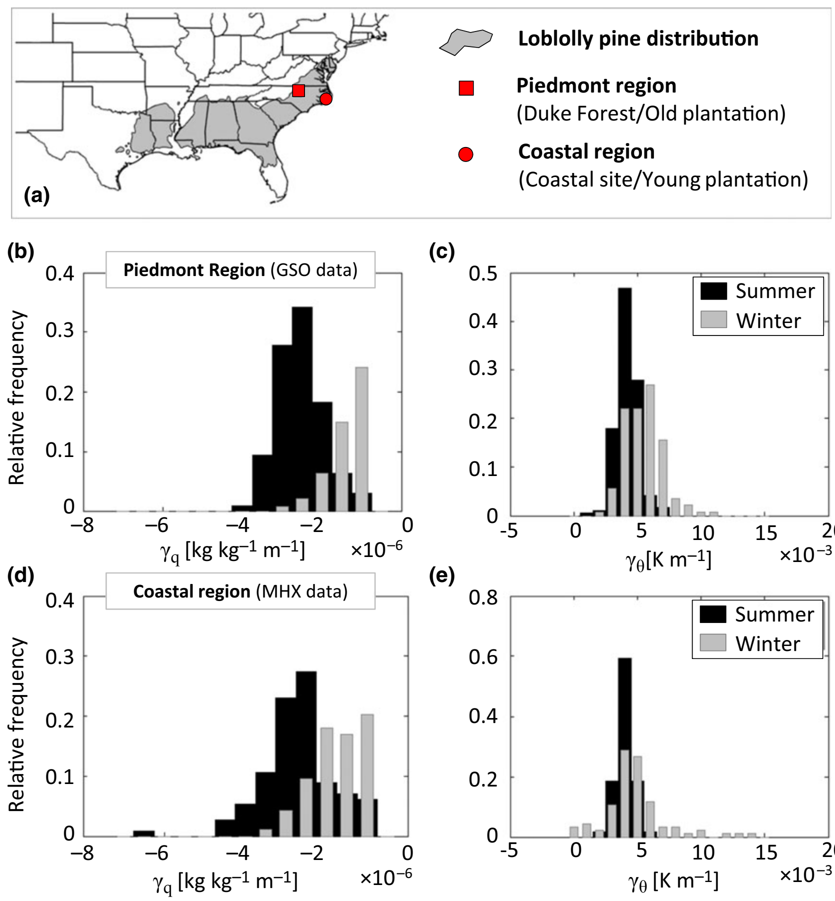

Fig. 1 Geographic distribution of Loblolly pines (*Pinus taeda* L.) in the southeastern USA (source: Little 1971) and location of the study sites (a). The sites are located in North Carolina, two in the Piedmont region (Duke Forest, Old plantation), and two in the Coastal region (Coastal site, Young plantation). Atmospheric parameters (temperature and specific humidity lapse rates γ_θ and γ_q) observed at the GSO airport (b, c) and at the MHX airport (d, e) during summer and winter periods.

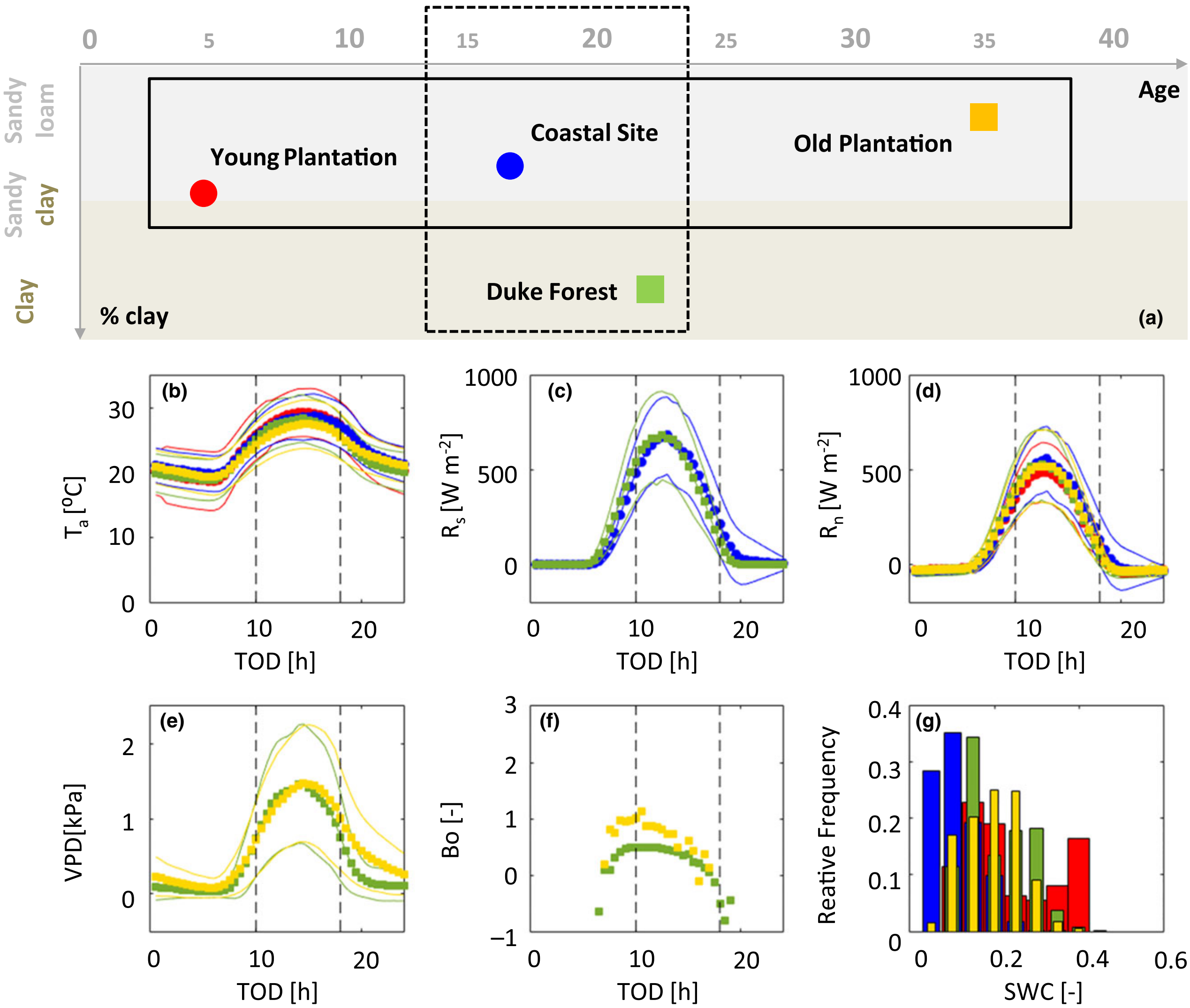

Fig. 2 Characteristics of the study sites and the interpretation of the multisite experiment: (a) soil texture, stand age, and (b–g) summertime (i.e., June–September) hydro-meteorological conditions. Temporal evolution (Time of Day, TOD) of (b) air temperature (T_a), (c) incoming shortwave radiation (R_s), (d) net radiation (R_n), (e) vapor pressure deficit (VPD, not available at the Coastal site/Young plantation), (f) Bowen ratio (Bo), and (g) relative frequency of soil water content (SWC) measured at the sites. In panels, b–f circles and squares represent ensemble averages for the study sites described in panel a (Coastal and Piedmont region, respectively), while solid lines are the ensemble averages $\pm$ a standard deviation. Dotted lines in panels b–f illustrate daytime conditions as defined in this study. The Young/Old plantation are used here as a chronosequence to evaluate age-related changes in the SPA conditions while the Coastal site/Duke Forest are used to evaluate the role of edaphic conditions.

(US-NC1 in the Ameriflux database) is near the Coastal site (4 km apart): it is an early rotation plantation that was clear-cut in 2004 and replanted in 2005 with 2-year-old loblolly pine seedlings. The dense understory during the first 2 years (2005–2007) was primarily composed of *Rubus ursinus* (blackberry), *Smilax rotundifolia* (greenbrier), and *Eupatorium capillofolium* (dog fennel) and reached a height of 2 m in 2009 (Domec *et al.*, 2012b). The soil is classified as Cape Fear Series fine, mixed, semiactive Typic Umbraquult. Eddy Covariance datasets and soil water content measurements were collected at the site as described elsewhere (Noormets *et al.*, 2010; Sun *et al.*, 2010; Domec *et al.*, 2012b). The Old plantation was a 35-year-old pine forest in the Piedmont region of North Carolina (NC), near the Duke Forest site (approximately 30 km northwest of the first study site). The Old stand was characterized by deep roots ($\sim$2 m deep) and a sandy loam soil (Oishi *et al.*, 2013), the understory was thinned in 1993 and 1998, and the canopy was quite sparse with a maximum LAI around 2.0 [m^2 m^{-2}], compared to $\sim$5.8 [m^2 m^{-2}] at the Duke Forest (see Table 1). Eddy covariance fluxes of sensible and latent heat were observed from 2003 to 2005 using an open-path gas analyzer (LI-7500; Li-Cor Biogeosciences, Licoln, NE, USA) and CSAT-3 sonic anemometer (Campbell Scientific, Logan, UT, USA) at a height of 33 m. Ancillary meteorological data

Table 1 Study sites: location, tree age, soil type, rooting depth, maximum leaf area index (LAI_{max}) and mean daytime (i.e., averaged between 10 am and 6 pm) net radiation (R_n) during the summer period

Site	Location	Stand age [year]	Data	Soil type	Root depth [m]	LAI_{max} [m^2 m^{-2}]	R_n [W m^{-2}]	Reference
Duke Forest	Durham, NC (USA)	22	2003–2005	Clay	0.3	5.8	440 ± 99	Stoy *et al.* (2005); Juang *et al.* (2007a)
Coastal site	Plymouth, NC (USA)	15	2007–2008	Histosol/Sandy loam*	1.9	5.6	468 ± 85	Sun *et al.* (2010); Domec *et al.* (2012b)
Young plantation	Plymouth, NC (USA)	2–5	2006–2009	Ultisol/Sandy loam†	0.9‡	4.1‡	430 ± 83	Domec *et al.* (2012b)
Old plantation	Alamance County, NC (USA)	35	2003–2005	Sandy loam	2.0	2.0	460 ± 110	Oishi *et al.* (2013)

*Sandy clay below 0.9 mbs (meters below surface), †Sandy clay below 0.6 mbs, ‡Measured in 2009.

included air temperature and relative humidity (HMP35C, Vaisala, Vanta, Finland), net radiation (CRN-4, Kipp & Zonen, Delft, the Netherlands), and photosynthetically active radiation (PAR, LI-190; Li-Cor). Data processing and quality control procedures are the same as those applied to the data from the 22-year-old site, as described in Stoy *et al.* (2006a,b). Root-zone soil moisture was also measured at the site (Oishi *et al.*, 2013). Further information on the Old plantation site can be found in Oishi *et al.* (2013). A summary of the characteristics of each study site is provided in Table 1. Here, we used measurements from 2003 to 2005 for the Duke Forest and the Old plantation, from 2007 to 2008 for the Coastal site, and from 2006 to 2009 for the Young stand.

The measurements from these sites are interpreted as follows: the Young plantation, the Coastal site, and the Old plantation are treated as a chronosequence so as to investigate the impact of tree age on partitioning of surface energy fluxes for similar soil texture conditions. We also use the Duke Forest and Coastal site of similar age to evaluate the role of different edaphic conditions on the partitioning of surface energy fluxes at a comparable age near-maximum productivity (Fig. 2a). The sites are all located in the same region and such site-intercomparison is performed to explore a wider range of variability in terms of both soil and age characteristics. The chronosequence is defined here as pine stands (same species) with different ages, but not necessarily located in the same location. They have comparable hydro-meteorological conditions and soil texture characteristics. As a matter of fact, a comparison of daytime ensemble averages of air temperature, incoming shortwave radiation (R_s), net radiation (R_n), and vapor pressure deficit (VPD) during summertime (i.e., June–September) demonstrates that the four study sites have statistically indistinguishable climatic conditions despite differences in geographic location and monitoring periods (Fig. 2b–e). Only minor differences in R_n among sites can be noted, and the influence of such differences on the model results is discussed in the next section. Also, while soil horizons differ at the study sites, root-zone soil hydraulic properties at the Young, Coastal, and Old sites are assumed here to be comparable: the soil type at the Young and Coastal plantations is organic matter over sandy loam (Domec *et al.*, 2012b) in the top 60 and 90 cm, respectively (i.e., where most of the roots are), similar hydraulic conductivities have been estimated for both sites (Diggs, 2004), and the estimated values are consistent with the typical hydraulic parameters of sandy loam (Old plantation). Possible implications of this assumption are discussed in the next section. Given the comparable climate, the Duke Forest/Coastal site are therefore chosen to evaluate the role of edaphic conditions (represented here by a clear difference in soil texture) on cloud formation mechanisms (Fig. 2a)

Daily midday sounding data from Greensboro (GSO) and Morehead/Newport (MHX) airports were used to estimate FA parameters at the Duke Forest/Old plantation and Coastal site/Young plantation, respectively. The temperature and specific humidity lapse rates γ_θ and γ_q were estimated using a linear regression analysis applied between $z \in [500, 5000]$ m. The datasets are divided into summer (June–September) conditions, when convective clouds are most common, and winter time (December–January) when shallow convection is not likely to occur. The FA parameters observed at the two sites are illustrated in Fig. 1. To estimate cloudiness at the sites, the Crawford and Duchon factor (Crawford & Duchon, 1999) is used as suggested elsewhere (Choi *et al.*, 2008) and is given by:

$$C = 1 - \frac{R_s}{R_{s0}}, \tag{1}$$

where R_s is the incident solar radiative flux density at the surface and R_{s0} is the theoretical clear-sky incident flux density. The diurnal evolution of R_{s0} is estimated by selecting a reference clear-sky day for each month of the year (using observations from the Coastal site and Duke Forest for the Coastal and Piedmont region, respectively). In this study, cloudiness is estimated only for days with low friction velocity ($u_* < 0.4$ [m s^{-1}]) and no rainfall. These two filters are applied to select days in which moisture advection in the atmosphere is not likely to play a dominant role in the cloud formation mechanism. Also, this u_* threshold ensures that the ABL growth is primarily driven by buoyant production of turbulent kinetic energy instead of mechanical production ($\propto u_*^3$). As the diurnal cycle of convection and cloud formation is of interest, daily averages of measured variables (e.g., radiation, latent, and sensible heat) are only calculated for daytime conditions (i.e., from 10 am to 6 pm).

Model formulation

The soil–plant–atmosphere (SPA) system is characterized by a number of state variables. For the atmospheric component, the following state variables are used: ABL height (h), ABL potential temperature (θ), ABL specific humidity (q), and LCL height ($\mathcal{L}$) all illustrated in Fig. 3. Assuming a linear profile of potential temperature and specific humidity in the FA (Porporato, 2009), the lapse rates γ_q and γ_θ are then used to define the FA state (Gentine *et al.*, 2013). In particular, the specific humidity lapse rate regulates the gradient of water vapor at the ABL top, thus controlling the entrainment of moist/dry air from the FA (Konings *et al.*, 2010; Gentine *et al.*, 2013; Bonetti *et al.*, 2015). The available energy (i.e., net radiation at the canopy top, R_n) is partitioned into latent (LE) and sensible (H_s) heat fluxes depending on the Bowen ratio (Bo $= H_s$/LE). The dynamics of h, air temperature, and humidity depends both on surface fluxes that are regulated by the soil–plant system and the entrainment fluxes at the ABL top. The latter fluxes are regulated by abiotic FA conditions that depend on synoptic scale variations instead of local surface conditions. The surface and FA regulations are encapsulated in the parameters Bo, γ_q and γ_θ. It is to be noted that specifying Bo is analogous to specifying the evaporative fraction EF $=$ LE/$R_n \approx$ LE/(LE $+ H_s$) $= (1 + \text{Bo})^{-1}$, which is common to the remote sensing and hydrology literature (e.g. Kustas *et al.*, 1993; Porporato, 2009; Gentine *et al.*, 2013).

In the simplified SPA model, the following assumptions are made: (A1) regional-scale convergence/divergence of heat and moisture are neglected and only vertical exchange is explicitly modeled; (A2) the ABL is well mixed; (A3) the Bo and EF are constant during the growth of h each day but can change from day to day; (A4) cloud formation can be approximated by the thermodynamic condition of saturation when the ABL and LCL heights cross. Literature data suggest that the Bowen ratio tends to remain nearly constant during midday hours and for well-watered conditions (e.g. Brutsaert & Sugita, 1992; Brutsaert & Chen, 1996; Brutsaert, 2005) because Bo is insensitive to the atmospheric conditions for large values of net radiation (Porporato, 2009). This is also confirmed by field observations from the Duke Forest and the Old plantation (Fig. 2f). Assumption A3 is therefore reasonable given that the model is employed here to describe morning/afternoon ABL dynamics under clear-sky conditions (i.e., when available energy is high). The influence of water stress on Bo occurs over longer time scales (i.e., day-to-day variations) and is implicitly accounted for through the Bo dependence on soil water content.

Assuming clear-sky net radiation varies according to a prescribed parabolic function of time t during the course of the day due to the large incident shortwave contribution, an analytical solution of the diurnal evolution of the ABL height h can be derived (Porporato, 2009) and is given by

$$h = \left[\frac{2}{3}\frac{(1+2\beta)\cdot R_{n,\max}\cdot \text{Bo}(3t_0 - t)\cdot t^2}{\rho\cdot c_p\cdot\gamma_\theta(1+\text{Bo})\cdot t_0^2}\right]^{1/2}, \tag{2}$$

where t_0 is the time at sunrise, $t_0 < t < 2t_0$ is the time of day, β is the fraction of sensible heat flux entrained from the top of the ABL (Tennekes, 1973), $R_{n,\max}$ is the daily maximum net radiation [W m^{-2}], γ_θ is the potential temperature lapse rate [K km^{-1}], $\rho = 1.29$ [kg m^{-3}] is the mean density of air, and $c_p =$ 1005 [J kg^{-1} K^{-1}] is the specific heat capacity of dry air at constant pressure. With the above assumptions, potential temperature and specific humidity in the ABL can be related to h as (Porporato, 2009):

$$\theta = \gamma_\theta\frac{1+\beta}{1+2\beta}\cdot h + \theta_{FA} \tag{3}$$

$$q = \gamma'_q\cdot h + q_{FA}, \tag{4}$$

where θ_{FA} and q_{FA} are the intercepts of the potential temperature and humidity linear vertical profiles, respectively, and γ'_q is a lapse rate for the humidity at the top of the mixed layer (Porporato, 2009):

$$\gamma'_q = \frac{1}{2}\left[\gamma_\theta\frac{c_p}{\lambda(1+2\beta)\text{Bo}} + \gamma_q\right] \tag{5}$$

where $\lambda = 2.45\times10^{-6}$ [J K^{-1}] is the latent heat of vaporization. The LCL height $\mathcal{L}$ is defined as (Stull, 1988)

$$\mathcal{L} = \frac{R\cdot\theta}{gM_a}\cdot\ln\left(\frac{P_s}{P_{LCL}}\right), \tag{6}$$

where $R = 8.314$ [J mol^{-1} K^{-1}] is the universal gas constant, g is the gravitational acceleration [m s^{-2}], M_a is the molecular weight of air ($\sim$29 g mol^{-1}), P_s [kPa] is the atmospheric pressure at the canopy surface, and P_{LCL} [kPa] is the atmospheric pressure at height $\mathcal{L}$, given by (Stull, 1988):

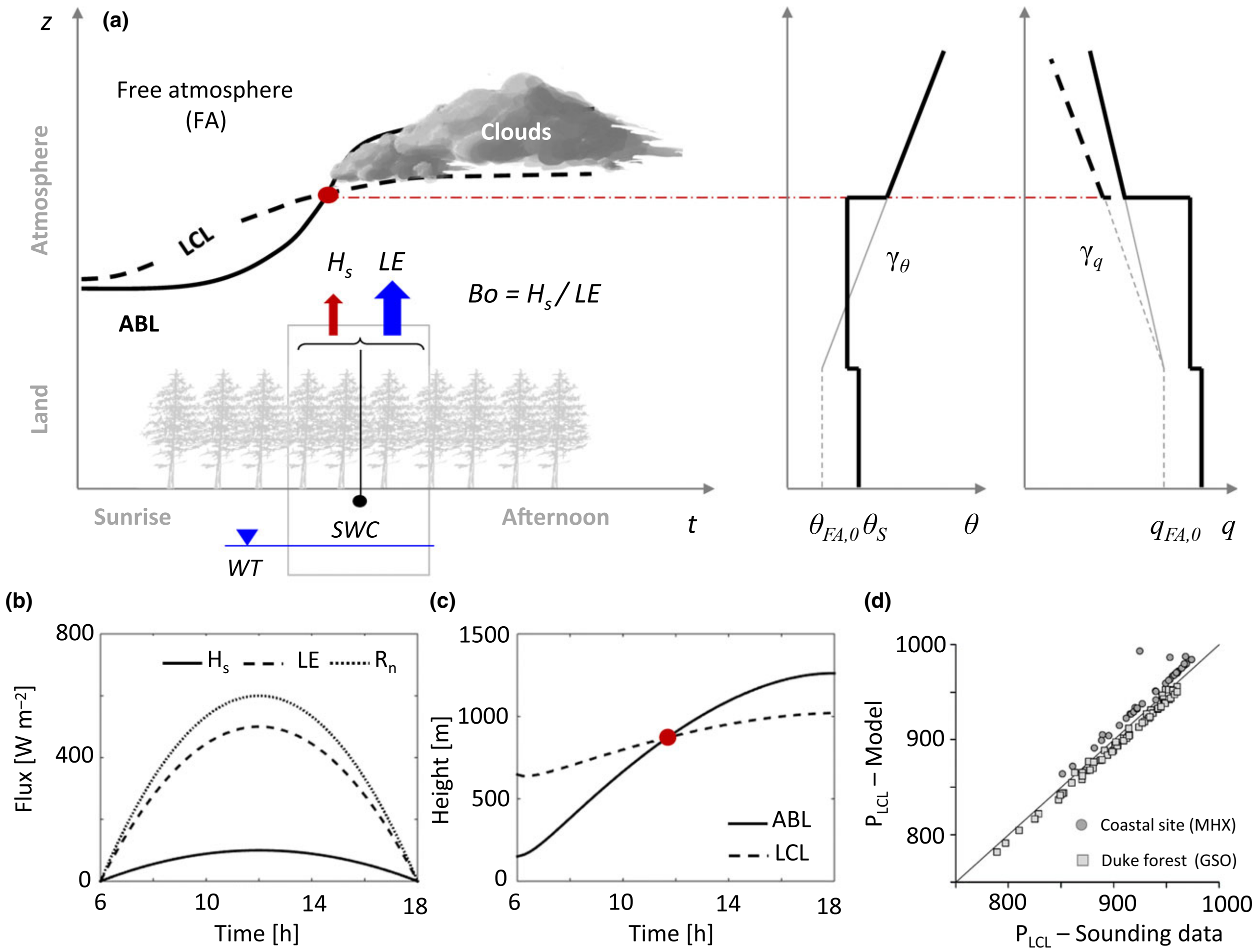

Fig. 3 Conceptual model: Soil–Plant–Atmosphere (SPA) system and potential temperature/specific humidity profiles (a). Diurnal variations of (b) latent and sensible heat fluxes for Bo = 0.2, $R_{n,max}$ = 600 [W m^{-2}], $\gamma_\theta = 4.0 \times 10^{-3}$ [K m^{-1}], $\gamma_q = -5.0 \times 10^{-6}$ [kg kg^{-1} m^{-1}] and (c) modeled ABL and LCL height. The ABL-LCL crossing is indicated by the dots in panel (a, d). A comparison between modeled and observed pressure at the LCL during June–July 2003 (GSO data) and 2007 (MHX data) is also shown (panel d).

$$P_{LCL} = P_s \left(\frac{\theta_{LCL}}{\theta}\right)^{3.5}, \quad (7)$$

where θ_{LCL} [K] is the saturation temperature at height $\mathcal{L}$ derived from the Clausius–Clapeyron equation as (Stull, 1988):

$$\theta_{LCL} = \frac{2840}{3.5 \cdot \ln(\theta) - \ln\left(\frac{rP_s}{0.622+r}\right) - 7.108} + 55, \quad (8)$$

where the near-surface atmospheric water vapor mixing ratio is $r \approx q$, and q is given by Eqn (4). Equations (2)–(8) provide a coupled description of ABL and LCL diurnal dynamics of the state variables $\{h(t), \theta(t), q(t), \mathcal{L}(t)\}$ once the external conditions are specified through $\Gamma = \{R_{n,max}, \gamma_\theta, \gamma_q\}$. The Bo encodes all the eco-physiological and soil–plant hydraulic controls on land-surface fluxes and is thus expected to vary, at minimum, with root-zone soil moisture. As an example, the modeled diurnal variations of surface energy fluxes and ABL and LCL heights are illustrated in Fig. 3b, c for a given set of parameters (Bo = 0.2, $R_{n,max}$ = 600 [W m^{-2}], $\gamma_\theta = 4.0 \times 10^{-3}$ [K m^{-1}], and $\gamma_q = -5.0 \times 10^{-6}$ [kg kg^{-1} m^{-1}]). A comparison between observed (from sounding data) and modeled P_{LCL} is also shown (Fig. 3d) to assess the LCL calculation. The evaluation was performed using June–July observations from both GSO and MHX airports.

Cloud formation

Assuming that the crossing of the lifting condensation level $\mathcal{L}$ and h results in the formation of convective clouds, we introduce the function:

$$\Delta(t, \Gamma) = h - \mathcal{L}, \quad (9)$$

and define a cloud formation criterion as:

$$\delta = sgn(\Delta(t, \Gamma)), \quad (10)$$

where $sgn(.)$ is the sign function (i.e., $sgn(x) = 1$ when $x > 0$ and $sgn(x) = -1$ when $x < 0$). Here, when $h > \mathcal{L}$, $\delta = 1$ and convective clouds develop at the ABL top. Conversely, clear-sky conditions occur when $h < \mathcal{L}$ or $\delta = -1$. Eqn (10) provides a measure of cloudiness and $\Delta(t, \Gamma) = 0.0$ (a surface in the space of the model external parameters) represents the transition from cloudy to cloudless conditions. Equation (9) can be solved numerically for t to derive the time of day t_c at which ABL and LCL cross, that is, $t_c = t|\Delta(t, \Gamma) = 0, t_0 < t < 2t_0$. The value of t_c represents the time of cloud occurrence and is relevant for practical applications (Gentine *et al.*, 2013). Alternatively, by noting that during a clear-sky day $\Delta(t, \Gamma) < 0\ \forall t < 2t_0$, the daily predisposition of the system to convective clouds can be described by $\Delta(2t_0, \Gamma) > 0$. The solution for $t = 2t_0$ is first presented and compared with the field measurements, then the time of cloud occurrence is discussed.

Results

Bowen ratio and cloud formation

The study ecosystems were predisposed to experience convective precipitation during the growing season, but not the dormant season, as illustrated in Fig. 4. The transition surface between cloudy ($\delta = 1$) and cloudless conditions ($\delta = -1$) as a function of surface fluxes (Bo) and the FA parameter γ_q, that is, the solution of $\Delta(2t_0, \Gamma) = 0$, is compared with the observed land-FA states at the two plantation sites during summer and winter conditions (but at different years). During the summer period, the data are clustered within the 'cloudy' region, and cloudiness tends to increase with distance from the manifold described by $\Delta = 0$ confirming the predisposition of both ecosystems to initiate convective clouds (as demonstrated by several studies (Juang *et al.*, 2007a; Konings *et al.*, 2010; Bonetti *et al.*, 2015)). To the contrary, due to the reduction in transpiration rates and evaporative fraction (higher Bo), winter conditions are not as likely to initiate convective clouds. The results in Fig. 4 are qualitative and not intended to capture all daily occurrences of fair-weather shallow cumuli. However, it can be safely stated that the results in Fig. 4 do provide a metric capable of determining 'predisposition' of ecosystems to initiate shallow convection – which is the necessary (but not sufficient) condition for rainfall occurrences.

Soil moisture and the Bowen ratio

In Fig. 5, sensible (H_s) and latent (LE) heat fluxes measured at the two sites and the corresponding values of

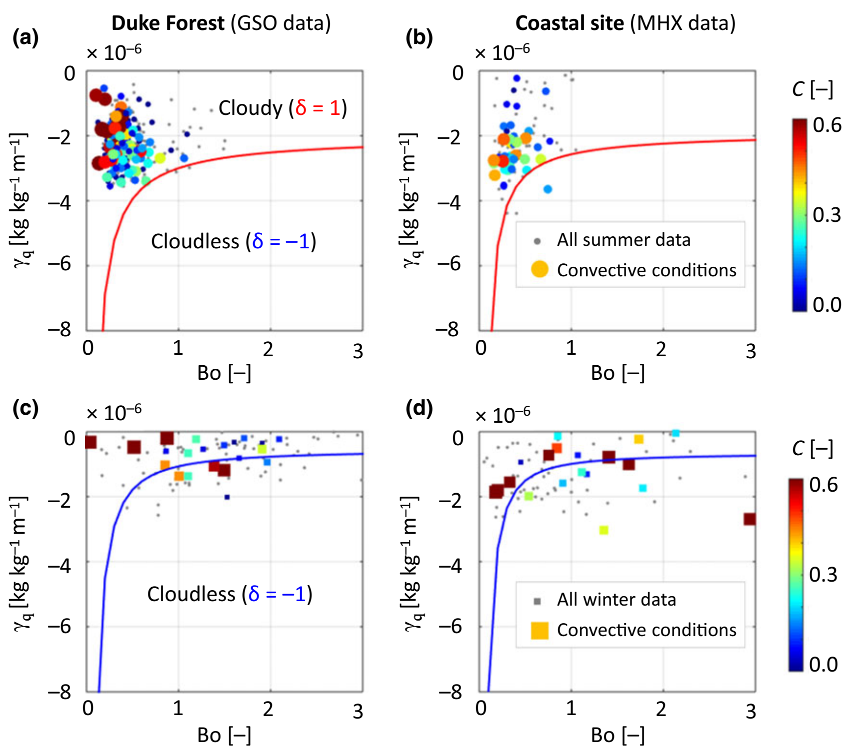

Fig. 4 Land-atmosphere conditions observed at Duke Forest and the Coastal site during summer (a, b) and winter (c, d). The solution of Eqn (9), indicating the transition from cloudy to cloudless conditions, is also shown (solid lines). Summer and winter runs with $R_{n,max} = 600$ W m^{-2} and $R_{n,max} = 300$ W m^{-2}, respectively, and mean summer and winter values of γ_θ extrapolated from Fig. 1c, e. The datasets were filtered to account for convective conditions only (see main text). All data points are shown for reference (gray dots).

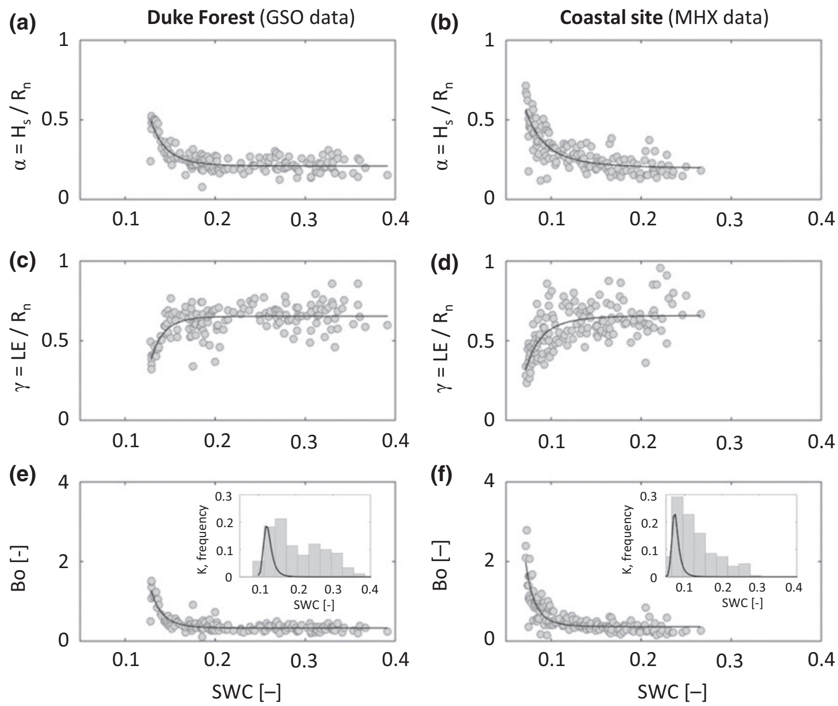

Fig. 5 Relation between surface energy fluxes (sensible heat H_s and latent heat LE normalized by net radiation R_n as in Juang *et al.* (2007b) and Bowen ratio Bo) and soil water content (SWC) observed at Duke Forest (a, c, e) and the Coastal site (b, d, f). The inset in panels (e) and (f) illustrates the relative frequency of soil moisture content during the summer months (bar plot) and the curvature K of the Bo−SWC relation (black line). Curvature is defined as: $K = |\frac{\partial^2 \mathrm{Bo}}{\partial^2 \mathrm{SWC}}| \cdot \left[1 + (\frac{\partial \mathrm{Bo}}{\partial \mathrm{SWC}})^2\right]^{-3/2}$.

the Bowen ratio have been plotted against measured root-zone soil water content (SWC). To minimize the effect of temperature, leaf area index (LAI) variations and precipitation on Bo, a subset of the data is constructed by selecting the following conditions: (i) no rain, (ii) $T_a > 10\,^{\circ}\mathrm{C}$, and (iii) $\mathrm{LAI} > 0.95 \cdot \mathrm{LAI}_{max}$, where LAI_{max} is the maximum LAI observed during the year. The first condition is needed because measured Bo is not accurate during and immediately following rain events (due to eddy covariance sensor wetness). The second condition ensures that the maximum carboxylation capacity of the pine foliage is sufficiently large so as to allow photosynthesis (and transpiration) to be significant (e.g., for $T_a < 8\,^{\circ}\mathrm{C}$, measured leaf photosynthesis for Loblolly pines is quite small (Katul *et al.*, 2010)). The third condition is selected for two reasons: to ensure that LAI dynamics are quasi-stationary (and near their maximum for summertime convective rainfall analysis) and to ensure that the forest floor evaporation is sufficiently small when compared to plant transpiration so that LE is primarily dominated by biotic factors (i.e., transpiration). The results in Fig. 5 provide a clear (albeit empirical) relation between Bo and SWC that is well approximated by a power law:

$$\mathrm{Bo(SWC)} = a \cdot \mathrm{SWC}^{-b} + \mathrm{Bo_w}, \qquad (11)$$

where a and b are parameters that depend on soil and vegetation characteristics and $\mathrm{Bo_w}$ is the Bowen ratio under well-watered conditions. These parameters clearly encode abiotic (e.g soil type) and biotic (e.g., plant water use efficiency) factors that can be linked to soil–plant hydraulics and ecophysiological properties by a number of mechanistic models with varying degrees of complexity (e.g.Williams *et al.*, 1996; Tuzet *et al.*, 2003; Siqueira *et al.*, 2008; Manoli *et al.*, 2014). However, for analytical tractability, the empirical Bo−SWC relation (Eqn 11) is used to illustrate how rooting depth and soil type (both coordinated in relation to climate (Guswa, 2008) and lumped in the parameters a and b) impact land surface energy fluxes.

Figure 5e, f demonstrates that a power law well represents the Bo−SWC observations at both sites. Such a relation bridges the complexity of root water uptake, stomatal regulation, and photosynthetic processes occurring within the SPA system and is consistent with observations from other ecosystems (Eltahir, 1998). The Duke Forest site exhibits an increase in Bowen ratio (i.e., transpiration becomes water-limited) at higher SWC values compared to the Coastal site, due to the clay soil texture and limited root-zone depth. Interestingly, at both sites, the mode of the SWC during summer conditions is close to the maximum curvature $K \propto |\frac{\partial^2 \mathrm{Bo}}{\partial^2 \mathrm{SWC}}|$ of the Bo−SWC relation (insets in Fig. 5e–f). The mode of SWC can be interpreted here as the 'operational' SWC pines experience most frequently. Despite the different soil types, the results in Fig. 5 demonstrate that the 'operational' summertime SWC of both ecosystems is close to, but slightly larger than the maximum value of the curvature K and for large SWC the Bowen ratio stabilizes at Bo ≈ 0.3 (i.e., $\frac{\partial \mathrm{Bo}}{\partial \mathrm{SWC}} = 0$). The maximum K curvature signals where a decrease in SWC induces a steeply increasing change in sensible heat flux (positive) and in latent heat flux (negative) due to the onset of soil water stress. These results suggest that both ecosystems maximize soil water use while minimizing Bo so that much of the available energy R_n is consumed in ET. When soil moisture declines so that Bo is no longer at its minimum, the increases in H_s and the maintenance of a reasonably high ET promote conditions conducive to convective rainfall occurrences. In other words, when mild soil moisture stress occurs and the root system cannot access additional water on short time scales relative to the root-growth time scales, these plantations appear to operate near a point where mild water stress conditions can favor rainfall predisposition. That is, on a short term (few days), this predisposition to rainfall may buffer against the onset of a persistent drought. These results agree with existing theories of a temporally positive and spatially negative soil moisture-precipitation feedback (Guillod *et al.*, 2015) and suggest some causal relation between dry and wet soil conditions. Here, we postulate that vegetation has the ability to passively 'switch' soil conditions from dry to wet states by sustaining convective precipitation also during dry soil conditions (negative coupling). This self-regulation mechanism coexists with the positive temporal correlation between ET and precipitation and can be partly attributed to stomatal control and leaf-level processes rather than root water uptake mechanisms. However, despite the active role of vegetation in the moisture recycling at the local scale, the generation of convective rainfall depends on ABL/LCL dynamics and regional moisture and pressure gradients (Katul *et al.*, 2012), rendering the vegetation-mediated feedback a secondary influence.

Soil moisture and cloud formation

The relation between surface energy fluxes and SWC reveals the role of soil conditions initiating cloud formation. Equation (11) can be used together with Equation (9) to define the cloud formation criterion as a function of soil moisture, that is, $\Delta(2t_0, \Gamma_{\mathrm{swc}}) > 0$, where $\Gamma_{\mathrm{swc}} = \mathrm{SWC}\gamma_q, \gamma_T$. The empirical Bo-SWC relation thus provides a cloudy–cloudless transition surface for different soil and FA conditions (by solving $\Delta(2t_0, \Gamma_{\mathrm{swc}}) = 0$ for γ_q). The results are illustrated in Fig. 6. For wet soil conditions, cloud formation can occur over a wider range of atmospheric parameters (with respect to dry conditions) due to the larger amount of water vapor transpired by vegetation (consistently with the results in Siqueira *et al.* (2009)). As the soil becomes drier, the moisture flux from the surface decreases (due to hydraulic controls) and shallow cumuli can form only if there is enough moisture entrained from the top of the ABL. The effect of water stress can be partly mitigated by a decrease in the temperature lapse rate that shifts the transition surface to lower values of γ_q (Fig. 6a, b). Note that changes in the temperature lapse rate are expected as a consequence of climate change and its role in the predicted increases in precipitation extremes is well known (O'Gorman & Scheider, 2009). Interestingly, the FA parameters observed at the study sites are in the range of values where changes in SWC can reduce the probability of convective clouds formation. However, for the period analyzed here, both ecosystems are reasonably well watered and support the formation of stratocumuli (as observed at the sites).

Age-related changes in the SPA conditions

The role of stand age in regulating the surface energy fluxes through the Bo−SWC relation is illustrated in Figs 7 and 8. These figures feature energy and water partitioning in the Young US-NC1 plantation, and in the Old North Carolina Piedmont plantation. In the Young plantation (2-year-old stand), the soil remains relatively wet after planting, the understory evaporation plays an important role (Domec *et al.*, 2012b), and stress conditions (increasing Bo) are observed for high values of SWC due to the shallow rooting systems of the young trees and the understory vegetation (Fig. 7). As the pines grow, the Bo value under well-watered conditions ($\mathrm{Bo_w}$) remains constant, but the 'operational' summertime SWC shifts toward drier conditions (Fig. 7e) approaching the maximum curvature of the Bo−SWC (that also shifts toward low SWC values). Stress conditions occur at lower SWC values as the root system of the pines develop and understory transpiration likely declines. Note that year 2007 and 2008 were characterized by severe droughts (Domec *et al.*, 2012b) as demonstrated by the low LE (high Bo) observed for the 3-year-old pines. By age 5, with more developed root system and canopy, the Young plantation begins

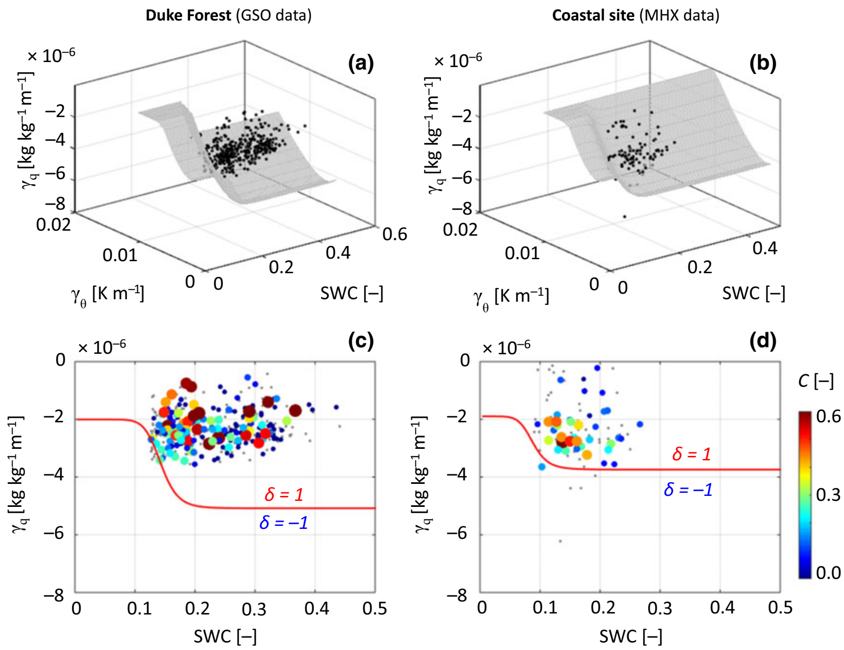

Fig. 6 Cloud formation surface (Δ = 0) compared with soil moisture and FA conditions (black dots) at Duke Forest (a) and the Coastal site (b) during summertime. In panels (c) and (d), cloudiness observed at the two sites is also shown (color bar). The transition from cloudy to cloudless conditions is illustrated by the cloud formation criterion δ (cloudy for δ = 1, cloudless for δ = –1). The datasets were filtered for convective conditions only (see main text). All data points are shown for reference (gray dots in panels c and d).

to exhibit Bo–SWC patterns similar to both the older Coastal and the Duke Forest sites. On the other hand, the Bowen ratio of the Old stand (Fig. 7b, d, f) shows little variations with the SWC and a much higher Bo_w value as compared to the Young plantation (see ΔBo_w in Fig. 7f). These results suggest that young pines (~ 2–5 years old) appear sensitive to soil conditions when compared to the Old stand (35 years old). With fully developed root system, the water use in mature trees appears limited only by their hydraulic conductivity (Noormets *et al.*, 2010). This results in their operating at the verge of hydraulic failure, but regional hydrology and site-level water recirculation mediated by vegetation provide sufficient moisture to sustain convective precipitation in all but the oldest stand. The land surface fluxes at the Old stand appear to be largely insensitive to soil moisture variations, which also imply low plant hydraulic conductivity and perhaps limited ability to recirculate available water (i.e., minimal K values, see Fig. 7e–f).

During the growth process, we observe a shift of summer SWC to dry conditions accompanied by a shift of the Bo–SWC relation that preserves possible self-regulation mechanisms (Fig. 8a, c). In other words, despite apparent water stress and partial cavitation, Bo and ET were maintained in a range conducive for convective rainfall. The Old stand was less sensitive to SWC variations (and drought) thus suggesting the existence of a stable state where surface energy fluxes are in equilibrium with the soil conditions via plant regulation (Fig. 8b, d). For the Old plantation, the range of SWC values that can influence cloud formation was limited and restricted to very dry conditions (Fig. 8d). These results suggest that in older stands (i) pines are less sensitive to drought, (ii) the partitioning of latent and sensible heat fluxes is weakly dependent on soil conditions, and (iii) the FA state plays a major role in triggering summer rainfall. Note however that a combination of low water holding capacity of the soil combined with the low LAI (see Table 1) could be contributing to the low evapotranspiration observed at the very old plantation.

Delzon & Loustau (2005) reported a decline in tree transpiration with age (for pines in the 10- to 91-year-old range), consistent with the Bo changes observed at the very old plantation. However, for the chronosequence in the Coastal region (i.e., Coastal site and Young plantation, 5–18 year old), an increase has been observed (Domec *et al.*, 2012b) suggesting that transpiration increases during the first stages of growth, reaches the maximum at maturity and then declines with further aging. In general, such age-related changes while impacting transpiration do not alter total ecosystem ET (Roberts, 1983; Delzon & Loustau, 2005), and as observed here, the LE fluxes are somewhat conserved.

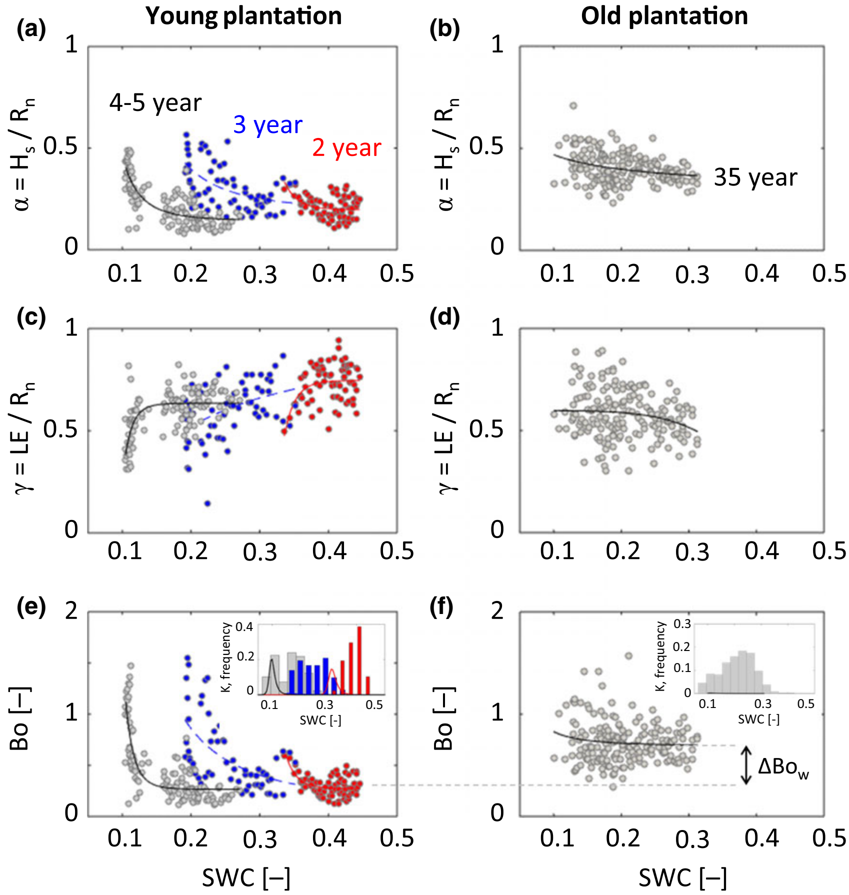

Fig. 7 Relation between surface energy fluxes and soil water content observed at the Young (a, c, e) and Old (b, d, f) plantations. The dataset from the Young plantation is divided into three subsets: year 2006 (2-year-old trees, red circles/line), year 2007 (3-year-old trees, blue circles/line), and years 2008–2009 (4- to 5-year-old trees, gray circle/black line). The inset in panels (e) and (f) illustrates the relative frequency of soil moisture content during the summer months (bar plot) and the curvature K of the Bo–SWC relation (black line).

Sensitivity analysis

Curvature K could be used as a metric of ecosystem sensitivity to drought, assuming that variations in net radiation across sites are small. Differences up to 20% in net radiation (R_n) between the Coastal site and the Young plantations were reported (Sun *et al.*, 2010) based on monthly/yearly averages. However, when considering summertime convective conditions only (i.e., high LAI), these difference drop to 6.5% and 3.5% for daytime (Table 1) and midday (Table 2) values, respectively. While small, these differences can still be attributed to age-related effects (e.g., changes in albedo and LAI) not captured in K. The purpose of this sensitivity analysis is to assess to what degree land-cover-induced variations in Bo and R_n impact land surface fluxes. Given the simplified energy balance $R_n = \mathrm{LE} + H_s$, the latent and sensible heat fluxes can be written as $\mathrm{LE} = \frac{R_n}{1+\mathrm{Bo}}$ and $H_s = \frac{\mathrm{Bo}}{1+\mathrm{Bo}} R_n$. The relative perturbation in the model output $\mathcal{O}$ (the surface fluxes) due to perturbations in the input parameters $\mathcal{P}_i$ (Bowen ratio and net radiation) can be written as $\frac{d\mathcal{O}}{\mathcal{O}} = \sum_i \frac{\partial \mathcal{O}}{\partial \mathcal{P}_i} \frac{d\mathcal{P}_i}{\mathcal{O}}$ to a leading order (Igarashi *et al.*, 2015), resulting in

$$\frac{d\mathrm{LE}}{\mathrm{LE}} = -\frac{d\mathrm{Bo}}{1+\mathrm{Bo}} + \frac{dR_n}{R_n}, \tag{12}$$

$$\frac{dH_s}{H_s} = \frac{d\mathrm{Bo}}{(1+\mathrm{Bo})\mathrm{Bo}} + \frac{dR_n}{R_n}. \tag{13}$$

The terms on the right side of Eqns (12) and (13) are evaluated for the case studies considering measured Bo and R_n differences among sites and between dry and wet soil moisture conditions (Table 2). The calculations are reported relative to the Old plantation and the dry state, respectively. The results demonstrate that perturbations in net radiation (dR_n) have a small (an order of magnitude difference) impact on LE and H_s variations ($\sim$0–3%) compared to Bo changes ($\sim$8–16% for LE, $\sim$11–23% for H_s). In 2009, the Young plantation received only 0.2% less radiation than the Old stand so that the changes observed in Fig. 7 can be entirely

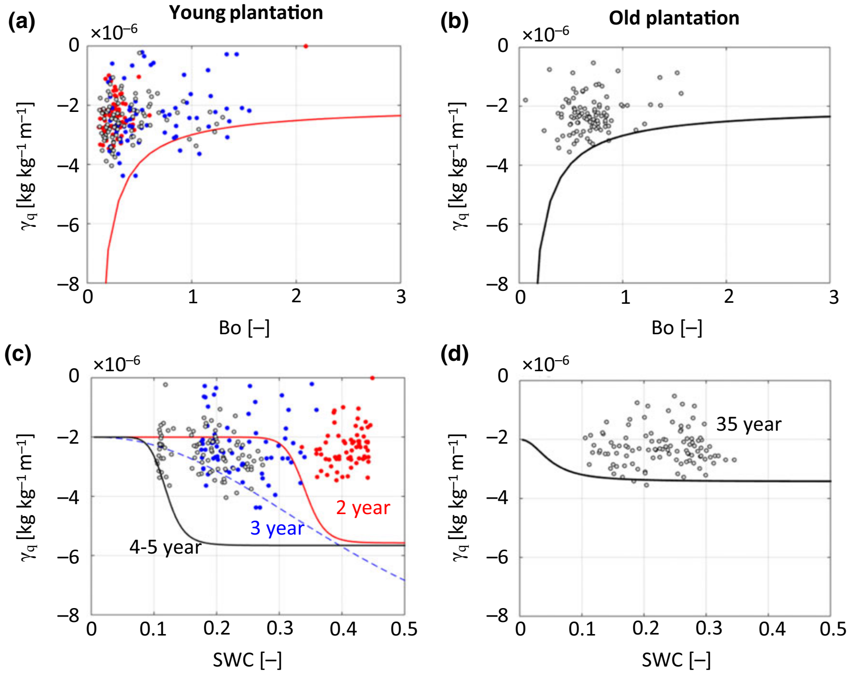

Fig. 8 Cloud formation surface (Δ = 0) compared with FA conditions, Bowen ratio (a, b) and SWC (c, d) at the Young (a, c) and Old (b, d) plantation during summertime. Colors in panels a and c refer to different stand ages as in Fig. 7.

Table 2 Sensitivity analysis: relative impact of Bo and R_n perturbations on the differences in latent and sensible heat fluxes (a) among sites and (b) between dry–wet conditions (relative to the Old plantation and the dry state, respectively) according to Eqns (12) and (13). Mean midday (i.e., averaged between 11 am and 2 pm) net radiation (R_n) values are considered in the calculations

	(a) Site–Old plantation			(b) Dry–wet conditions*		
Site	$-\frac{d\text{Bo}}{1+\text{Bo}}$ [%]	$\frac{d\text{Bo}}{(1+\text{Bo})\text{Bo}}$ [%]	$\frac{dR_n}{R_n}$ [%]	$-\frac{d\text{Bo}}{1+\text{Bo}}$ [%]	$\frac{d\text{Bo}}{(1+\text{Bo})\text{Bo}}$ [%]	$\frac{dR_n}{R_n}$ [%]
Duke Forest	16.8	−23.4	−3.5	29.4	−33.8	−12.5
Coastal site	8.1	−11.3	3.3	47.0	−31.5	10.3
Young plantation†	16.3	−22.6	−0.2	29.5	−40.3	7.4
Old plantation	–	–	–	3.9	−5.0	−6.7

*Dry conditions: SWC < 0.15 (0.08 for the Coastal site), wet conditions: SWC > 0.2; †2009 data.

attributed to age-related effects explained by Bo (assuming similar soil texture and hydroclimatic conditions). In general, the impact of Bo variations is stronger on H_s than LE, consistent with the observed key role of Bo in regulating the growth of the ABL. As demonstrated by previous studies, LE fluxes at the ecosystem level are generally conserved (Roberts, 1983; Delzon & Loustau, 2005) because changes in tree transpiration with stand age are partly compensated for by the understory contribution. The influence of H_s changes on Bo thus play a major role in controlling ABL dynamics. The results in Table 2 also show that the changes in Bo between wet and dry conditions are higher than R_n perturbations for young/mature trees, but they become comparable at the Old stand, confirming that old trees are more tolerant to drought (Delzon & Loustau, 2005; Domec *et al*., 2012b).

Discussion

The effect of vegetation on convective cloud formation

The results presented in the previous sections provide one single measure to determine the ecosystem and FA conditions initiating shallow convection over pine plantation ecosystems. We have shown that the Bowen ratio is regulated by complex land-vegetation feedback mechanisms which depends on a plethora of both biotic (plant hydraulic and stomatal conductance) and abiotic (e.g., soil water availability) processes, effectively encoding the effects of land surface energy partitioning on convective cloud formation. The analysis made use of the fact that summertime variations in daytime Bowen ratio (or evaporative fraction) are small when compared to the fast dynamics of the ABL and day-to-day variations in Bowen ratio mainly reflect soil moisture stress on the soil–plant system. The conceptual model in Fig. 3 can be quantitatively described by Eqn (9) and used to determine how soil and vegetation feedbacks ultimately impact boundary layer cloud formation (Fig. 9a–d). The same general mechanistic control on convective cloud formation would hold in other ecosystems and can be used to evaluate the effects of land-use and land-cover change on regional water availability as mediated by surface energy partitioning. For example, a reduction in latent heat fluxes will result in a delayed formation of clouds and decreased probability of convective rainfall events (Fig. 9). In contrast, reforestation or transitions from very old natural pine forests to young fast growing plantations (as being projected for the SE) may enhance summertime clouds, thus supporting surface cooling (Jackson *et al.*, 2008). Changes in the shape of the Bo–SWC thus provide a quantitative metric to evaluate the effects of age-related land-cover changes on regional cloud formation and rainfall recycling mechanisms. The cloud formation model developed here (Eqns 9-10, Fig. 9) suggests that variations in soil water availability can produce 'abrupt' transition from cloudy to cloudless conditions. The level of water stress the vegetation experiences can reduce the pine transpiration and drive the ecosystem to a suppression of convective clouds. The threshold for the onset of water stress thus provides a threshold for convective cloud formation and lack of subsequent precipitation might enhance water stress through a positive feedback mechanism (i.e., less transpiration, less precipitation). Such threshold is shown to depend on both soil characteristics and stand age, suggesting that pines development stage can influence the ability of the SPA system to recirculate available water (see conceptual illustration in Fig. 9d). This finding suggests some degree of self-regulation within the hydrologic cycle of young pine stands. Note, however, that only convective processes are considered and such changes can be mitigated, at least in the short term, by frontal systems (or a more extreme version, hurricanes). Very old pine

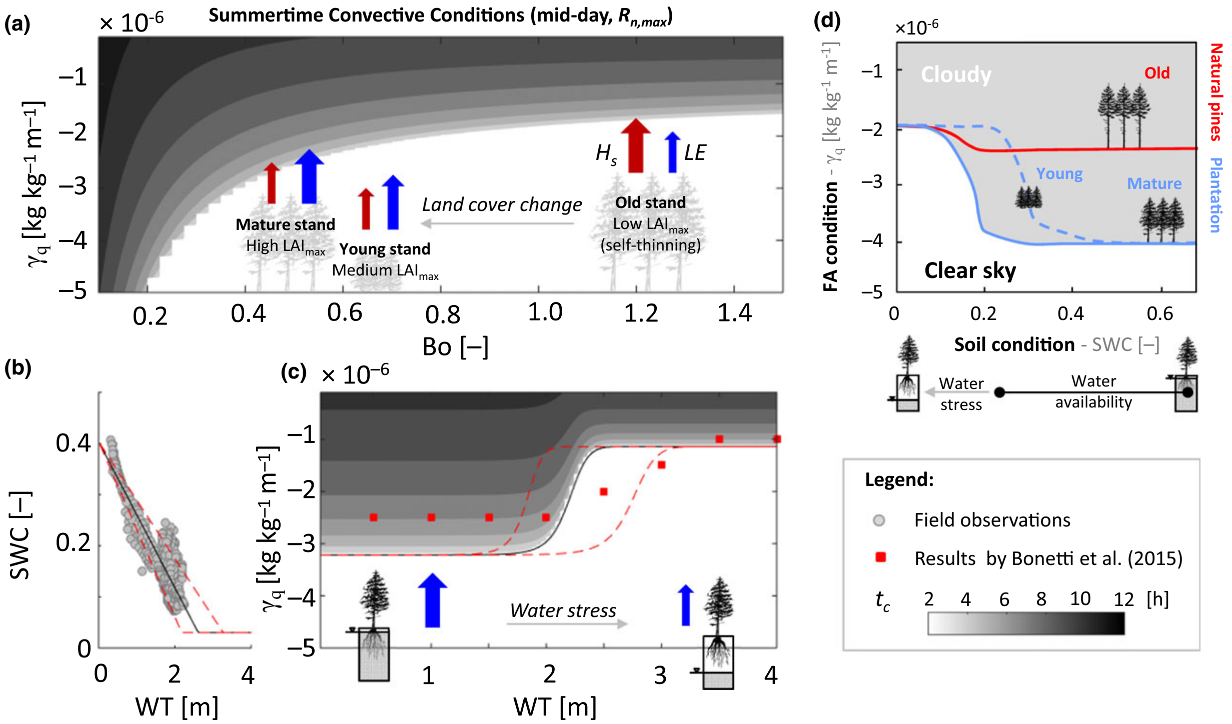

Fig. 9 Cloud formation function Δ (continuous line) and time of cloud occurrence t_c (gray scale) as a function of (a) Bowen ratio and (c) water table depth (WT) for a given net radiation R_n (600 W m^{-2}). An empirical linear relation is used to relate WT to soil moisture content at the Coastal site (b). The approximated solution Δ = 0 is compared with the results of numerical simulations presented in Bonetti *et al.* (2015) (red squares in panel c). Given the uncertainties in the WT–SWC relation, different interpolation lines have been tested (dotted lines in panels b and c). A schematic representation of age-related effects on soil–plant–atmosphere conditions regulating convective cloud formation is presented in panel d.

stands are less sensitive to drought due to deeper rooting and self-thinning over time. This result is consistent with mature broadleaf stands, which exhibit conservative water use and are fairly resistant to drought (Oishi *et al.*, 2010; Novick *et al.*, 2015).

The ability of the proposed zero-dimensional approach to capture land-surface feedback mechanisms is now assessed by comparing the cloud formation function (Eqn 9) with results of a detailed SPA model recently developed by Bonetti *et al.* (2015) for the Coastal site. To this purpose, the SWC variations at the Coastal site are converted into water table depth (WT) variations (illustrated in Fig. 9b), which were previously used to drive the simulations by the complex SPA model (Bonetti *et al.*, 2015). The numerical model by Bonetti *et al.* (2015) employs Richards equation to describe soil moisture redistribution in three dimensions, 3D root water uptake as regulated by a stomatal optimization model with a dynamic marginal water use efficiency, and a surface energy balance coupled with a slab representation of ABL-LCL dynamics. Comparing the solution of Eqn (9) with the results of this detailed numerical model (red squares in Fig. 9c) shows that the two approaches broadly agree on the sensitivity of the coastal pine plantation system to the same range of FA and soil moisture conditions initiating convective Clouds. The two curves in Fig. 9b are shifted due to the oversimplified representation of the connection between water table variations and SWC (explicitly resolved in the complex SPA model).

The results in Fig. 9 are also consistent with several monitoring (e.g. Eltahir, 1998; Freedman *et al.*, 2001) and modeling (e.g. Kollet & Maxwell, 2008; Sanchez-Mejia & Papuga, 2014; Bonetti *et al.*, 2015) studies. The well-known interplay between surface energy fluxes and shallow stratocumuli formation has been confirmed here. In addition, explicit connections with FA and soil moisture status have been unfolded by the model developed. The model results support previous conclusions regarding the positive correlation between groundwater depth, sensible heat fluxes (Kollet & Maxwell, 2008), and ABL height (Sanchez-Mejia & Papuga, 2014). In addition, the relative importance of land-surface vs. FA conditions has been analytically disentangled thereby allowing clear separation between key biotic and abiotic controls regulating the transition from cloudy to cloudless regimes using analytical expressions.

Study limitations

Our analysis considered only four sites with similar climatic but different edaphic locations. Also, data from different monitoring periods were analyzed. These choices were dictated by the need to explore a wide range of stand ages (from 2-year-old up to $\sim$ 35-year-old pines) and soil textures, but the assumption of comparable edaphic and hydroclimatic conditions introduces some uncertainties. Here, soil texture was used as a proxy for comparing sites with similar/different edaphic conditions assuming that soil hydraulic characteristics were comparable and played the major role in regulating SPA interactions. However, soil characteristics were not exactly the same and other soil properties (e.g., pH, soil nitrogen) may have differed among sites, thus influencing the observed plant–water relations. Such differences can exist also at the stand level but their impact on the partitioning of surface energy fluxes at large scales have been ignored. Another main limitation of this study is the use of a single very old stand where fluxes were available for similar soil texture and hydro-climatic conditions. A part for the young pines at very early stages of growth (i.e., 2–3 year old), the observed Bo−SWC relations showed a comparable trend across three of four study sites (increasing Bo for decreasing SWC at the Young Plantation, the Coastal site, and the Duke Forest, that is, pines in the range of 5–22 year old) and only the Old Plantation ($\sim$35 year old) demonstrates a clear deviation. Additional datasets from older (i.e., > 35 year old) pine stands are required to confirm the robustness of the observed age-related differences. Finally, the assumption of a constant Bowen ratio during the day, while necessary to derive the analytical solution in Eqn (2), is not valid in general (especially during very early morning and later afternoon). Variations of Bo at shorter temporal scales (e.g., hourly) may introduce complex ABL dynamics that are partly responsible for day-to-day variations in cloud occurrence. The same is true for FA conditions (assumed constant during the day as well).

Broader impacts

The leading eco-hydrologic mechanisms governing the transition between cloudy–cloudless regimes over the land surface appear to be encoded in the nonlinearity between the Bowen ratio Bo (or alternatively, evaporative fraction) and root-zone soil water content, SWC. The precise shape of this nonlinearity is governed by site water availability, plant hydraulic conductance, and transpiring leaf area that affect the partitioning of available energy into sensible and latent heat fluxes. The work here showed that for high SWC, $\frac{\partial \mathrm{Bo}}{\partial \mathrm{SWC}} \approx 0$ and Bo $\approx$ 0.3 across different sites (Loblolly pine plantations from 2 to 22 years old), irrespective of soil type or rooting zone depth. With declining SWC, the Bowen ratio increased and convective cloud formation was suppressed when a threshold SWC (that depends on the soil/roots characteristics) was reached. However, the 'operational' summertime SWC was found (at these sites) close to such a threshold, corresponding to the SWC over which the curvature $K \propto |\frac{\partial^2 \mathrm{Bo}}{\partial^2 \mathrm{SWC}}|$ is maximum. These findings suggest that these forest ecosystems operate at the cusp of hydraulic failure through much of the growing season, while still supporting high enough transpiration rates to trigger convective cloud formation and local hydrologic recycling.

At the regional scale, age-related changes in the ecosystem heat and moisture fluxes can modify cloud cover and alter the precipitation regime. In the southeastern USA, the current FA conditions lie in a zone where the Bo−SWC conditions can impact convective cloud formations thereby making land-cover change (from older pine forests to younger and faster growing plantations as suggested by recent economic projections (Wear & Greis, 2002; Juang *et al.*, 2007b)) an issue in water resources. Such impacts can be amplified (or mitigated) by both climate- and human-induced changes. The predicted temperature increase is expected to increase the atmospheric vapor pressure deficit (Delucia *et al.*, 2001) with direct effects on the evapotranspiration fluxes. Modeling studies also suggest that the increase of atmospheric CO_2 can modify the existing Bo−SWC relations (e.g. de Arellano *et al.*, 2012), but recent observations demonstrate that elevated CO_2 is likely to have little influence on canopy transpiration (Tor-ngern *et al.*, 2015).

On the other hand, given the large scale of land-cover changes in the southeastern US (31% of its forest cover was either lost or gained following short-cycle tree planting and harvesting (Hansen *et al.*, 2013)) population growth (United States Census Bureau, 2005) and plantation forestry expansion (Wear & Greis, 2012) projected for the region can impact boundary layer processes by affecting subsurface water availability and land surface fluxes. The work here shows that depletion of groundwater may lead to reductions in convective precipitation in regions where root-zone soil moisture is regulated by water table variations, resulting in a positive feedback on the depletion process.

Acknowledgements

This study was supported by the National Science Foundation (NSF-EAR-1344703) and the US Department of Energy through the Office of Biological and Environmental Research Terrestrial Carbon Processes program (DE-SC0006967 and DE-SC0011461). US-NC1 and US-NC2 flux sites have been supported by DOE BER-TES awards number 7090112 and 11-DE-SC-0006700, USDA NIFA CAP Award 2011-68002-30185, and USDA Forest Service Eastern Forest Environmental Threat Assessment Center Grant 08-JV-11330147-038. The authors confirm that they have no interest or relationship, financial, or otherwise that might be perceived as influencing objectivity with respect to this work.

References

de Arellano JVG, van Heerwaarden CC, Lelieveld J (2012) Modelled suppression of boundary-layer clouds by plants in a CO_2-rich atmosphere. *Nature Geoscience*, **5**, 701-704.

Baker JB, Langdon GO (1990) Loblolly pine (*Pinus taeda* L.). In: *Silvics of North America. Volume 1, Conifers*, Agricultural Handbook 654 (eds Burns RM, Honkala BH), pp. 497–512. USDA Forest Service, Washington DC.

Ban-Weiss GA, Bala G, Cao L, Pongratz J, Caldeira K (2011) Climate forcing and response to idealized changes in surface latent and sensible heat. *Environmental Research Letters*, **6**, 034032.

Bonetti S, Manoli G, Domec JC, Putti M, Marani M, Katul G (2015) The influence of water table fluctuations and the free atmospheric state on convective rainfall predisposition. *Water Resources Research*, **51**, 2283–2297.

Brutsaert W (2005) *Hydrology: An Introduction*. Cambridge University Press, Cambridge, 605 pp.

Brutsaert W, Chen D (1996) Diurnal variation of surface fluxes during thorough drying (or severe drought) of natural prairie. *Water Resources Research*, **32**, 2013–2019.

Brutsaert W, Sugita M (1992) Application of self-preservation in the diurnal evolution of the surface energy budget to determine daily evaporation. *Journal of Geophysical Research*, **97**, 18377–18382.

Choi M, Jacobs JM, Kustas WP (2008) Assessment of clear and cloudy sky parameterizations for daily downwelling longwave radiation over different land surfaces in Florida, USA. *Geophysical Research Letters*, **35**, L20402.

Churkina G, Schimel D, Braswell BH, Xiao X (2005) Spatial analysis of growing season length control over net ecosystem exchange. *Global Change Biology*, **11**, 1777–1787.

Crawford TM, Duchon CE (1999) An improved parameterization for estimating effective atmospheric emissivity for use in calculating daytime downwelling longwave radiation. *Journal of Applied Meteorology*, **38**, 474–480.

Delucia EH, Maherali H, Carey EV (2001) Climate-driven changes in biomass allocation in pines. *Global Change Biology*, **6**, 587–593.

Delzon S, Loustau D (2005) Age-related decline in stand water use: sap flow and transpiration in a pine forest chronosequence. *Agricultural and Forest Meteorology*, **129**, 105–119.

Diggs JA (2004) Simulation of nitrogen and hydrology loading of forested fields in Eastern North Carolina using DRAINMOD-N 11. MSc thesis, North Carolina State University, Raleigh, NC, 155 p.

Domec JC, Ogée J, Noormets A *et al.* (2012) Interactive effects of nocturnal transpiration and climate change on the root hydraulic redistribution and carbon and water budgets of southern United States pine plantations. *Tree Physiology*, **32**, 707–723.

Domec JC, Sun G, Noormets A, *et al.* (2012b) A comparison of three methods to estimate evapotranspiration in two contrasting loblolly pine plantations: age-related changes in water use and drought sensitivity of evapotranspiration components. *Forest Science*, **58**, 497–512.

Driedonks AGM (1982) Models and observations of the growth of the Atmospheric Boundary Layer. *Boundary-Layer Meteorology*, **23**, 283–306.

Eltahir, EAB (1998) A soil moisture-rainfall feedback mechanism: 1. Theory and observations. *Water Resources Research*, **4**, 765–776.

Findell KL, Eltahir EAB (2003) Atmospheric controls on soil moisture-boundary layer interactions: feedbacks within the continental United States. *Journal of Hydrometeorology*, **4**, 570–583.

Frederick WJ, Lien SJ, Courchene CE, DeMartini NA, Ragauskas AJ, Iisa K (2008) Production of ethanol from carbohydrates from loblolly pine: a technical and economic assessment. *Bioresource Technology*, **99**, 5051–5057.

Freedman JM, Fitzjarrald DR, Moore KE, Sakai RK (2001) Boundary layer clouds and vegetation atmosphere feedbacks. *Journal of Climate*, **14**, 180–197.

Friend AD, Arneth A, Kiang NY, *et al.* (2007) FLUXNET and modelling the global carbon cycle. *Global Change Biology*, **13**, 610–633.

Gentine P, Ferguson CR, Holtslag M (2013) Diagnosing evaporative fraction over land from boundary-layer clouds. *Journal of Geophysisical Research: Atmospheres*, **118**, 8185–8196.

Guillod BP, Orlowsky B, Miralles DG, Teuling AJ, Seneviratne SI (2015), Reconciling spatial and temporal soil moisture effects on afternoon rainfall. *Nature Communications*, **6**, 6443.

Guswa AJ (2008) The influence of climate on root depth: a carbon cost-benefit analysis. *Water Resource Research*, **44**, W02427.

Hansen MC, Potapov PV, Moore R, *et al*. (2013) High-resolution global maps of 21st-century forest cover change. *Science*, **342**, 850–853.

Igarashi Y, Katul GG, Kumagai T, *et al*. (2015) Separating physical and biological controls on long-term evapotranspiration fluctuations in a tropical deciduous forest subjected to monsoonal rainfall. *Journal of Geophysical Research: Biogeosciences*, **120**, 1262–1278.

Jackson R, Randerson J, Canadell J et al. (2008) Protecting climate with forests. *Environmental Research Letters*, **3**, 044006.

Juang JY, Porporato A, Stoy PC et al. (2007a) Hydrologic and atmospheric controls on initiation of convective precipitation events. *Water Resources Research*, **43**, W03421.

Juang JY, Katul G, Porporato A et al. (2007b) Eco-hydrological controls on summertime convective rainfall triggers. *Global Change Biology*, **13**, 1–10.

Katul GG, Manzoni S, Palmroth S, Oren R (2010) A stomatal optimization theory to describe the effects of atmospheric CO_2 on leaf photosynthesis and transpiration. *Annals of Botany*, **105**, 431–442.

Katul GG, Oren R, Manzoni S, Higgins C, Parlange MB (2012) Evapotranspiration: a process driving mass transport and energy exchange in the soil-plant-atmosphere-climate system. *Reviews of Geophysics*, **50**, RG3002.

Kim CP, Entekhabi D (1998) Feedbacks in the land-surface and mixed-layer energy budgets. *Boundary-Layer Meteorology*, **88**, 1–21.

Kollet SJ, Maxwell RM (2008) Capturing the influence of groundwater dynamics on land surface processes using an integrated, distributed watershed model. *Water Resources Research*, **44**, W02402.

Konings AG, Katul G, Porporato A (2010) The rainfall-no rainfall transition in a coupled land convective atmosphere system. *Geophysical Research Letters*, **37**, L14401.

Koster RD, Dirmeyer PA, Guo Z et al. (2004) Regions of strong coupling between soil moisture and precipitation. *Science*, **305**, 1138–1140.

Kustas WP, Schmugge TJ, Humes KS et al. (1993) Relationships between evaporative fraction and remotely sensed vegetation index and microwave brightness temperature for Semiarid Rangelands. *Journal of Applied Meteorology and Climatology*, **32**, 1781–1790.

Little EL (1971) Atlas of united states trees, volume 1, conifers and important hardwoods, *Tech. rep.* U.S. Department of Agriculture Miscellaneous Publication 1146.

Manoli G, Bonetti S, Domec JC, Putti M, Katul G, Marani M (2014) Tree root systems competing for soil moisture in a 3d soil-plant model. *Advances in Water Resources*, **66**, 32–42.

Maxwell RM, Chow FK, Kollet SJ (2007) The groundwater-land-surface-atmosphere connection: soil moisture effects on the atmospheric boundary layer in fully-coupled simulations. *Advances in Water Resources*, **30**, 2447–2466.

Noormets A, Gavazzi MJ, McNulty SG, Domec JC, Sun G, King JS, Chen JQ (2010) Response of carbon fluxes to drought in a coastal plain loblolly pine forest. *Global Change Biology*, **16**, 272–287.

Novick KA, Oishi AC, Ward EJ, Siqueira M, Juang JY, Stoy PC (2015) On the difference in the net ecosystem exchange of CO_2 between deciduous and evergreen forests in the southeastern United States. *Global Change Biology*, **21**, 827–842.

O'Gorman PA, Scheider T (2009) The physical basis for increases in precipitation extremes in simulations of 21st-century climate change. *Proceedings of the National Academy of Sciences*, **106**, 14773–14777.

Oishi CA, Oren R, Novick KA, Palmroth S, Katul G (2010) Interannual invariability of forest evapotranspiration and its consequence to water flow downstream. *Ecosystems*, **13**, 421–436.

Oishi CA, Palmroth S, Butnor JR, Johnsen KH, Oren R (2013) Spatial and temporal variability of soil CO2 efflux in three proximate temperate forest ecosystems. *Agricultural and Forest Meteorology*, **171–172**, 256–269.

Oren R, Ewers BE, Todd P, Philips N, Katul G (1998) Water balance delineates the layer in which soil moisture affects canopy conductance. *Ecological Applications*, **8**, 990–1002.

Pino D, de Arellano JVG, Kim SW (2006) Representing sheared convective boundary layer by zeroth- and first-order-jump mixed-layer models: large-eddy simulation verification. *Journal of Applied Meteorology and Climatology*, **45**, 1224–1243.

Porporato A (2009) Atmospheric boundary-layer dynamics with constant bowen ratio. *Boundary-Layer Meteorology*, **137**, 227–240.

Ramírez-Cobo P, Lee KS, Molini A, Porporato A, Katul G, Vidakovic B (2011) A wavelet-based spectral method for extracting self-similarity measures in time-varying two-dimensional rainfall maps. *Journal of Time Series Analysis*, **32**, 351–363.

Roberts J (1983) Forest transpiration: a conservative hydrological process? *Journal of Hydrology*, **66**, 133–141.

Salvucci GD, Saleem JA, Kaufmann R (2002) Investigating soil moisture feedbacks on precipitation with tests of Granger causality. *Advances in Water Resources*, **25**, 1305–1312.

Sanchez-Mejia ZM, Papuga SA (2014) Observations of a two-layer soil moisture influence on surface energy dynamics and planetary boundary layer characteristics in a semiarid shrubland. *Water Resources Research*, **50**, 306–317.

Schäfer KV, Oren R, Ellsworth DS, *et al*. (2003) Exposure to an enriched CO_2 atmosphere alters carbon assimilation and allocation in a pine forest ecosystem. *Global Change Biology*, **10**, 1378–1400.

Schalkwijk J, Jonker HJJ (2013) Simple solutions to steady-state cumulus regimes in the convective boundary layer. *Journal of the Atmospheric Sciences*, **70**, 3656–3672.

Siqueira M, Katul G, Sampson DA, Stoy PC, Juang JY, McCarthy HR, Oren R (2006) Multiscale model intercomparisons of CO_2 and H_2O exchange rates in a maturing southeastern US pine forest. *Global Change Biology*, **12**, 1189–1207.

Siqueira M, Katul G, Porporato A (2008) Onset of water stress, hysteresis in plant conductance, and hydraulic lift: scaling soil water dynamics from millimeters to meters. *Water Resource Research*, **44**, W01432.

Siqueira M, Katul G, Porporato A (2009) Soil moisture feedbacks on convection triggers: the role of soil-plant hydrodynamics. *Journal of Hydrometeorology*, **10**, 96–112.

Stevens B (2006) Bulk boundary-layer concepts for simplified models of tropical dynamics. *Theoretical and Computational Fluid Dynamics*, **20**, 279–304.

Stoy PC, Katul G, Siqueira M et al. (2005) Variability in net ecosystem exchange from hourly to inter-annual timescales at adjacent pine and hardwood forests: a wavelet analysis. *Tree Physiology*, **25**, 887–902.

Stoy PC, Katul G, Siqueira M, Juang JY, Novick KA, Uebelherr JM, Oren R (2006a) An evaluation of models for partitioning eddy covariance-measured net ecosystem exchange into photosynthesis and respiration. *Agricultural and Forest Meteorology*, **141**, 2–18.

Stoy PC, Katul G, Siqueira M et al. (2006b) Separating the effects of climate and vegetation on evapotranspiration along a successional chronosequence in the southeastern U.S. *Global Change Biology*, **12**, 1–21.

Stull RB (1988) *An Introduction to Boundary Layer Meteorology*. Springer, New York.

Sun G, Noormets A, Gavazzi MJ et al. (2010) Energy and water balance of two contrasting loblolly pine plantations on the lower coastal plain of North Carolina, USA. *Forest Ecology and Management*, **259**, 1299–1310.

Taylor MC, de Jeu RAM, Guichard F, Harris PP, Dorigo WA (2012) Afternoon rain more likely over drier soils. *Nature*, **489**, 423–426.

Tennekes H (1973) A model for the dynamics of the inversion above a convective boundary layer. *Journal of the Atmospheric Sciences*, **30**, 558–567.

Tennekes H, Driedonks AGM (1981) Basic entrainment equations for the atmospheric boundary layer. *Boundary-Layer Meteorology*, **20**, 515–531.

Tor-ngern P, Oren R, Ward EJ, Palmroth S, Mccarthy HR, Domec JC (2015) Increases in atmospheric CO_2 have little influence on transpiration of a temperate forest canopy. *New Phytologist*, **205**, 518–525.

Tuzet A, Perrier A, Leuning R (2003) A coupled model of stomatal conductance, photosynthesis and transpiration. *Plant Cell & Environment*, **7**, 1097–1116.

United States Census Bureau (2005) 2005 Interim State Population Projections. Available at: https://www.census.gov/ (accessed 20 February 2015).

Wear DN, Greis JG (2002) Southern forest resource assessment. gen. tech rep. srs-53, *Tech. rep.* US Department of Agriculture, Forest Service, Southern Research Station, Asheville, NC.

Wear DN, Greis JG (2012) The Southern Forest Future Project: Summary Report. Gen. Tech Rep. SRS-168. *Tech. rep.* US Department of Agriculture, Forest Service, Southern Research Station, Asheville, NC.

Wei J, Dickinson R, Chen H (2008) A negative soil moisture precipitation relationship and its causes. *Journal of Hydrometeorology*, **9**, 1364–1376.

Williams M, Rastetter EB, Fernandes DN, et al. (1996) Modelling the soil plant atmosphere continuum in a *Quercus–Acer* stand at Harvard Forest: the regulation of stomatal conductance by light, nitrogen and soil/plant hydraulic properties. *Plant Cell & Environment*, **19**, 911–927.

Williams CJR, Allan RP, Kniveton DR (2012) Diagnosing atmosphere–land feedbacks in CMIP5 climate models. *Environmental Research Letters*, **7**, 044003.

Wu W, Dickinson R, Wang H, Liu Y, Shaikh M (2007) Covariabilities of spring soil moisture and summertime United States precipitation in a climate simulation. *International Journal of Climatology*, **27**, 429–438.